OPTIMAL BUCKLING DESIGN OF A COMPOSITE PLATE OPERATING IN A GIVEN TEMPERATURE RANGE

Luis Henrique de Andrade
Departamento Logístico (Divisão Técnica – DLog/QGEx) – CEP 70630-901, Brasília – DF, Brazil
E-mail: henrique@dlog.eb.mil.br

Sérgio Frascino Müller de Almeida
Instituto Tecnológico de Aeronáutica
Address: 12228-900 São José dos Campos, SP, Brazil
E-mail: frascino@mec.ita.cta.br

José Antônio Hernandes
Instituto Tecnológico de Aeronáutica
Address: 12228-900 São José dos Campos, SP, Brazil
E-mail: hernandes@aer.ita.br

Abstract:
Thermal residual stresses are usually present in composite plates and may strongly affect their critical buckling load. The complexity of the structural analysis problem demands the use of optimization techniques to properly design laminates that consider the effects of residual thermal stresses. These effects when appropriately taken into account for a given temperature can enhance plate mechanical behavior. However, a design that is optimal for a certain temperature may perform poorly at another operating temperature. In practice, an aircraft part must perform satisfactorily in any temperature within a certain operation temperature range. In this work, an efficient algorithm is applied to maximize the buckling load of a laminated plate within a given temperature range, taking into account the residual thermal stress effects. The layer thicknesses are taken as design variables to optimize the buckling load factor of a composite laminated plate of fixed mass. The structural analysis is based on a finite element model and linearized buckling loads are obtained by solving the corresponding eigenvalue problem. Analytical sensitivity analysis is used with respect to the design variables. The optimal designs obtained are insensitive to temperature changes inside the pre-assigned temperature range, with a complex thickness distribution that maximizes the critical buckling load and simultaneously neutralizes the deleterious effects of the thermal residual stresses.

Keywords: *Structural optimization, buckling loads, composite plates, thermal residual stresses.*

1. Introduction

Thermal residual stresses due to the cure or consolidation process are always present in polymeric composite structures due to the distinct thermal expansion coefficients of the fiber and resin. Almeida and Hansen (1997) pointed out that the resultants of thermal residual stresses may be non-zero for stiffened thin composite plates and introduced the idea of taking advantage of these residual stresses to improve the structural response in critical buckling load problems. Andrade (2002) developed an optimization tool and used approximation concepts to maximize the structural performance of such plates in eigenproblems. Optimization of the plate critical buckling load with the proposed approach was performed at a reduced computational cost.

In a first attempt, Andrade, Almeida and Hernandes (2001) optimized the buckling response considering a given optimization temperature, which should coincide with the intended plate operation temperature. However, this approach has its shortcomings since the optimal design obtained for a fixed optimization temperature may behave poorly for some other operation temperature. An aircraft typically operates in a temperature range between -54^{o}C and 65^{o}C (Almeida and Santacreu, 1995); therefore, its parts must perform satisfactorily for any temperature within this range. When solved by current available optimization tools, in the context of finite element analysis and mathematical programming, this design optimization problem would certainly require a huge computational effort, when compared to other optimization tasks, due to typical difficulties of convergence when the objective is eigenvalue maximization.

This work proposes a new approach to the structural optimization of composite plates within a given temperature range, taking into account the residual thermal stress effects, based on the concepts developed by Andrade (2002). The optimization tool applied to the present problem has as its main characteristics the computational efficiency, which is achieved by performing a small number of complete structural finite element analyses in the search for the optimal design.

2. Finite Element Plate Buckling Eigenproblem

The composite plate with stiffeners is analyzed using a Reissner-Mindlin formulation. The plate is assumed to be symmetrical with respect to its mid-surface such that there is no coupling between membrane and bending behavior.

The finite element method is used for modeling the plate. A Lagrangian bi-cubic isoparametric element with 16 nodes was implemented in a FORTRAN code (Almeida and Hansen, 1997). The element has 5 degrees of freedom (u, v, w, y_x, y_y) per node with a total of 80 degrees of freedom per element. The element is free of shear locking effects being applicable to thin as well as to thick plates (Hepler and Hansen, 1986).

The eigenvalues and eigenvectors of the system equations is the solution for the elastic stability problem described by:

$$\left(\underset{\approx}{K} + \underset{\approx\, G}{K^R} - l_m \underset{\approx\, G}{K^0} \right) \underset{\sim}{f}_m = \underset{\sim}{0} \tag{1}$$

where l_m are the eigenvalues, $\underset{\approx}{K}$ is the global stiffness matrix, $\underset{\approx\, G}{K^R}$ is the geometric stiffness matrix due to the in-plane thermal residual stresses and $\underset{\approx\, G}{K^0}$ is the geometric stiffness matrix associated to a given in-plane pre-buckling loading (prescribed displacement at one edge of the plate).

3. Structural Optimization

The design variables are the heights X_i of the lamina, measured downwards from the plate midsurface. A constant total mass constraint is used to keep the plate mass equal to its initial value. Constraints are imposed on the design variables to force an inner height to be smaller than an outer one within any group of design variables associated to the same laminate region. Design variable limits are also imposed.

The main solution strategy (Andrade 2002) consists of the identification of the critical mode among the set of active modes in a given optimization cycle. The active modes are the lower ones that are close within a given tolerance to the fundamental mode. At the beginning, one of the active modes is used as the critical one, to which an eigenvalue Rayleigh quotient approximation is associated and it is made the problem objective function, while lower limit constraints are imposed on each of the remaining eigenvalues associated to the active modes. The process is in such a way that any of the active modes can become the objective function whereas modal constraints are imposed on the others. This approach is herein called *critical mode identification strategy – CMIS* (Andrade, 2002).

The Rayleigh quotient approximations (Canfield, 1990) are used in order to construct explicit approximations for the objective function and constraints belonging to the active set. The CMIS strategy is therefore in the framework of the Approximation concepts approach (Schmit and Miura, 1976), where the optimal solution is sought through the optimization of a sequence of approximate subproblems.

For all examples, the convergence criterion is assumed to be satisfied when the relative difference between the values of the objective function at the end of a complete optimization cycle and the previous is $0.0 \leq \varepsilon \leq 0.1\%$ for two consecutive iterations. The percentage of global reduction for the design variables move limits is 12% (Thomas et all, 1992). The adopted individual increment for the design variables is 33%. The individual increment is activated when an upper or lower bound is reached for a design variable in two consecutive optimization cycles.

4. Buckling Load Otimization for a Temperature Range

The finite element model used to represent a simply supported orthotropic composite plate is shown in Fig.(1). The plate is square, such that $a = b = 360$ *mm*. It is subject to a prescribed uniform displacement, d, applied to its top edge, in the y axis direction. The material properties assumed for a 0.15*mm* thick carbon/epoxy T300/5208 layer are (Andrade, 2002):

- Elastic longitudinal modulus, $E_1 = 154500$ MPa;
- Elastic transversal modulus, $E_2 = 11130$ MPa;
- Poisson's ratio (inplane), $n_{12} = 0.304$;
- Shear modulus (inplane), $G_{12} = 6980$ MPa;
- Shear modulus (transverse), $G_{13} = 6980$ MPa;
- Shear modulus (transverse), $G_{23} = 3360$ MPa;
- Specific mass, $r = 1.56 \times 10^3$ kg/m^3;
- Longitudinal thermal expansion coefficient, $a_1 = -0.17 \times 10^{-6}$ /$^\circ$C;
- Transverse thermal expansion coefficient, $a_2 = 23.1 \times 10^{-6}$ /$^\circ$C.

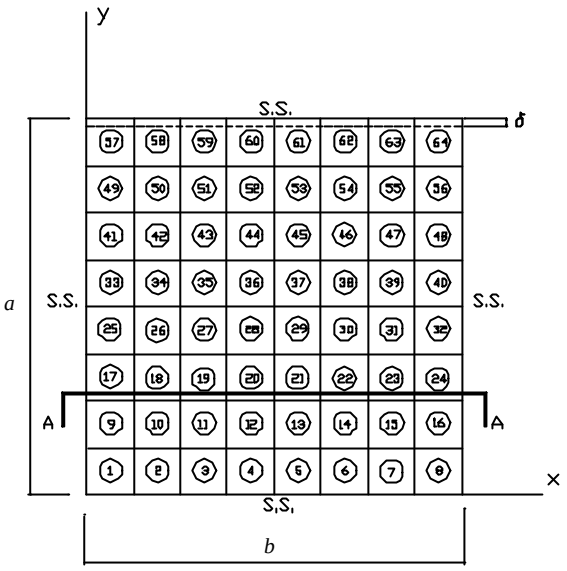

Figure 1 – Finite element plate mesh with 64 elements subjected to prescribed displacement, *d*.

The temperature range is assumed to be from DT = -150°C to DT = 0°C. When DT = 0°C, the structure is operating at the cure temperature. The stacking sequence of the initial plane plate is $[(0/90)_2]_s$. Its critical buckling parameter is l_1 = 2.65 for the applied edge displacement d = 0.003*mm*.

4.1 Design Variables

The design variables are the heights reinforcing plies along the direction of the applied displacement. Figure (2) shows the plate cross section where the design variables, X_1 to X_8, are represented in the lower half of the plate. The strips in Fig. (2) represent regions that have different thicknesses. Those regions are refereed to as stiffeners due to its discrete nature. It is important to remark that the plate is symmetrical with respect to the *z* axis. These variables have lower limits equal to half of the base plate thickness. The base plate has a uniform constant thickness and is formed by the inner lamina; the base plate is not allowed to change during optimization.

The lamination angles in Fig.(2) are measured from the *x* axis. Therefore, the 90° plies have the fiber direction aligned with the loading as the prescribed pre-buckling displacements are applied along the *y* direction. The 0° plies have the fiber orientation transverse to the prebuckling load.

Variables X_1 and X_2 control the heights of two identical parallel stiffeners defined by elements 4, 12, 20, 28, 36, 44, 52, 60 and 5, 13, 21, 29, 37, 45, 53, 61, respectively (Fig.1). Variables X_3 and X_4 control the heights of the two stiffeners in the *y* direction defined by the top elements 59 thru 62; similarly X_5 and X_6, for stiffeners corresponding to top elements are 58 and 63; finally, X_7 and X_8 control the stiffeners located along the edges.

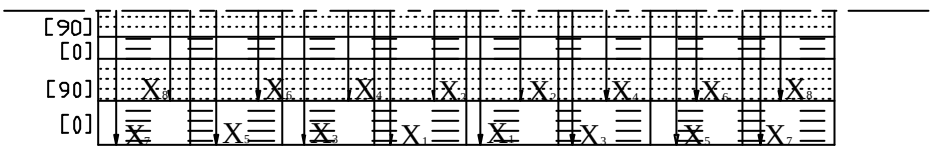

Figure 2 – Design variables used for the longitudinal stiffeners.

4.2 Plate Optimization at a Given Temperature (Approach #1)

Initially, the temperature interval is divided into an arbitrary number of smaller intervals. As an example, three intervals with four *DT's* equally spaced are used in the analyses. For each *DT* the optimal design is obtained using the *critical mode identification strategy* (*CMIS*). Two mode constraints are applied in addition to the side variables and mass constraints used in all optimizations. The critical load values of the optimal designs for different *DT's* are then normalized with respect to the critical load of the uniform plate - initial project for all optimizations - with the same

mass that the optimized plates. The activation range includes modes with eigenvalues within 40% above the value of the fundamental eigenvalue computed in the base design.

Figure (3) contains the curve of maximized and normalized fundamental eigenvalues for each design corresponding to each chosen temperature (*DT's* = 0ºC, -50ºC, -100ºC and -150ºC), equally spaced within 0ºC to -150ºC range. The plot clearly shows the stiffening effect of the thermal residual stresses increasing the buckling load. The curve that interpolates the four points is nearly a straight line, except for the small inflection at *DT* = -100ºC. Figure (4) displays the reinforcements thickness distribution for the optimal designs obtained for different *DT's*. The figure scale along the thickness direction is multiplied by 20 with respect to the horizontal dimensions to improve the visualization of layer orientations and thicknesses.

The algorithm seeks optimal design variables that maximize the buckling load at a specific operation temperature. Thus, as Fig.(4) demonstrates, the optimal design variables are different for different *DT's*.

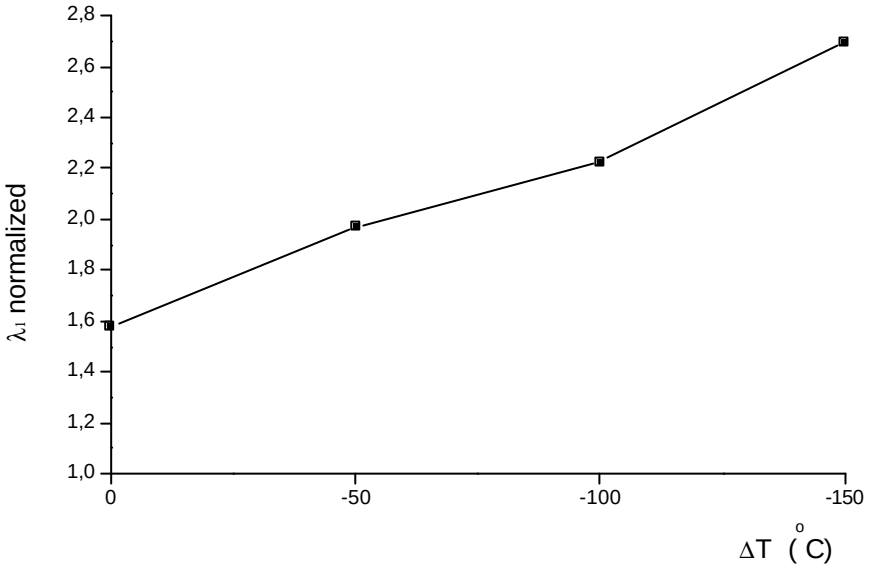

Figure 3 – Normalized $l_1^{[ot]}$*'s* computed for each different *DT*.

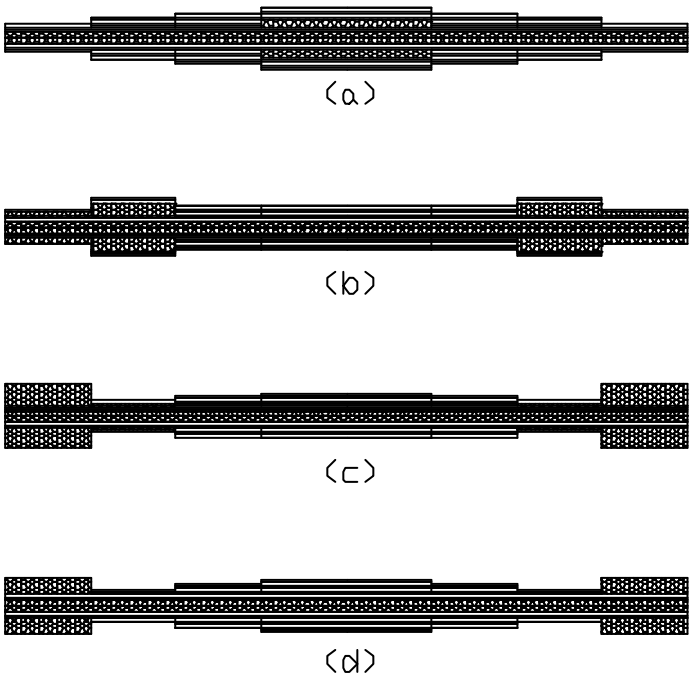

Figure 4 – Thickness distributions of the optimal designs for (*a*) *DT* = 0°C, (*b*) *DT* = -50°C, (*c*) *DT* = -100°C and (*d*) *DT* = -150°C.

It can be observed in Fig.(4) that the optimal design for *DT* = 0ºC concentrates layers at 0º and 90º in the two central stiffeners; those are the thickest stiffeners in the plate. The other stiffeners present only 0º layers with decreasing thickness towards the free edges of the plate. The stiffeners are actually eliminated at the edges. For *DT* = -50ºC, the reinforcement arrangement [0/90] appears in the two stiffeners adjacent to edge on each side of the plate. The inner stiffener is thicker than the one at the edge. The internal area of the plate just presents stiffeners with 0º layers.

It can be verified from Fig.(4c) that for *DT* = -100ºC thick reinforcements composed only of 90º layers are located at the edges, whereas the internal adjacent stiffeners present thin [0/90] arrangements. The stiffeners of the internal plate area are thin, composed only of 0º layers, and with nearly uniform thickness. Finally the design for *DT* = -150ºC possesses the same thick 90º stiffeners at edges and internal stiffeners with only 0º orientation. The differences of thickness of those stiffeners are larger than those observed at the optimal design for *DT* = -100ºC.

As it will be verified, the optimum design obtained for a certain *DT* cannot be - and frequently it is not - the best design for another *DT*, different from that for which it was optimized. This fact raises an important issue: which is the best design of a structure that operates in a range of temperatures?

To verify the performance of a design optimized in a reference temperature when operated at another one, structural analyses were accomplished for the four reference *DT's* in the operation range, for each one of the optimal configurations obtained. The correspondents fundamental eigenvalues are plotted in Fig.(5).

It must be remarked that each curve in Fig.(5) refers to the same optimal project, analyzed in different reference temperatures. It should be expected that the maximum eigenvalue for each reference temperature be that corresponding to the optimal design for this temperature. In Fig.(5), this happens for three reference temperatures, *DT* = 0ºC, -50ºC and -150ºC, however for *DT* = -100ºC the maximum eigenvalue corresponds to that one of optimum design *DT* = -150ºC rather than the optimum design for *DT* = -100ºC. This was caused by the convergence difficulty observed in the problem for *DT* = -100ºC. Although the obtained results are close, the optimal design for *DT* = -100ºC cannot be qualified strictly as an optimum point.

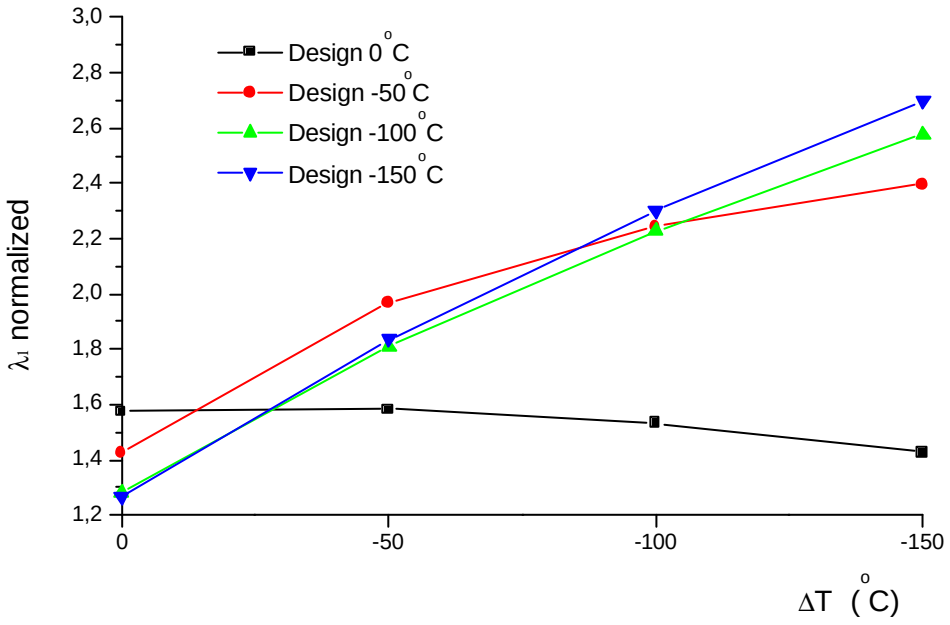

Figure 5 – Optimal projects applied in different operation temperatures.

4.3 Integrated Optimization within the Temperature Range (Approach #2)

In this section as well as in the next the *critical mode identification strategy – CMIS* (Andrade, 2002) is applied to the optimization problem of a plate that should operate within a temperature range. The problem that seeks the maximization of the laminate plate buckling load factor can be briefly stated, according to the *CMIS*, as:

$$\max_{r} \max_{h_r} l_{1(\Delta T_r)}, \qquad r = 1, 2, ..., n_D \tag{2}$$

$$s.t. \quad 1 - \frac{l_{1(DT_i)}}{l_{1(DT_R)}} \le 0, \qquad i = 1, 2, ..., n_{DT}, \quad i \neq R \tag{3}$$

The design variables are the lamina heights h_r, for which side constraints are applied, but here omitted for the sake of brevity. Equation (2) imposes the choice of the largest maximum among the optimal solutions obtained for each one of the reference temperatures. Equation (3) imposes constraints that the fundamental eigenvalues of other reference temperatures be greater than that maximized for the temperature DT_r.

The *CMIS* is well adapted to the solution of the problem stated above (Andrade, 2002). In the previous section, *CMIS* was applied to consider as active modes for a specific reference temperature *DT* those inside of a band of tolerance. The critical mode is chosen among those to determine the optimal solution. Now, in the context of several reference temperatures, the process is basically the same, except that the potentially critical modes are not associated to only one but to different reference temperatures DT_r.

The solutions of the eigenvalue problems obtained from the structural analyses in each reference temperature DT_r are used to build explicit approximations in the design variables for the objective functions and design constraints to be used in the sequence of approximate subproblems.

For each one of the reference temperatures, the n_m first modes are tested to decide whether to take part or not of the group of potentially critical modes. For all examples in this work, the band for mode activation of 40% is adopted.

The curves corresponding to numeric results of the studied problem are depicted in Fig(6). It can be observed that the solution obtained for the proposed problem leads to a design that has critical eigenvalues greater than the one for the initial plate with constant thickness for all four reference temperatures. Those eigenvalues vary slightly for different reference temperatures, being practically constant within the temperature range considered. Consequently the obtained optimal solution has the virtue of providing the same level of structural safety in the whole temperature range.

It is worth noticing that the flexibility obtained with the *CMIS* approach in allowing critical mode changes yields higher results for $l_1^{[ot]}$ in the optimal solution of this project with operational requirement of range of temperatures. The application of a simple optimization strategy based just in the application of mode restrictions leads to significantly poorer $l_1^{[ot]}$ results (Andrade, 2002).

4.4 Integrated Optimization within the Temperature Range with Eigenvectors for only one *DT* (Approach #3)

It can be observed in Fig.(3) that, for a certain design, the fundamental eigenvalues vary approximately in a linear way with temperature. This can be explained through the Rayleigh quotient. In such equation, the geometric stiffness matrix corresponding to thermal residual stresses acting on the plate, obtained from thermal forces and moments in the laminates, is proportional to the temperature difference *DT*. Assuming the simplifying hypothesis that the eigenvectors are invariant for finite changes in the design variables, the eigenvalues would be linear functions of *DT*. It is known that the eigenvectors invariance hypothesis leads to good results in problems with design variables of cross section dimensions,. However, it should be pointed out that eventually the temperature variation can cause a significant change in the fundamental mode resulting in a strongly non-linear relation between the critical load and the temperature in the neighborhood of the considered design point. This type of difficulty will be overcome by the use of the *CMIS* strategy.

The almost linear dependence of the critical eigenvalue with the temperature difference is the motivation for the development of an optimization strategy slightly different from the one in the previous section. This strategy explores the idea of generating explicit approximations for the eigenvalues not only in terms of the design variables but also in terms of temperature thus avoiding eigenproblem solutions for all reference temperatures. This strategy allows the optimization in the whole range of prescribed temperature using only the structural analysis for one of the reference temperatures, called the base temperature. The statement of the typical subproblem based on the strategy delineated in this section is identical to that already used in the previous section, with the exception that the approximation for the eigenvalues is based on the design variables and reference temperature DT_r.

Similarly to the previous case, to become a candidate to be the objective function of an optimization subproblem, the approximate eigenvalue in a reference temperature DT_r should be within in the activation band of 40%. This band is computed with respect to the smallest approximate fundamental eigenvalue obtained among all the reference temperatures of the base design. Also as the previous strategy (approach #2), this approach guarantees that the eigenvalue chosen as objective function, which is maximized, will be the smallest within the operation temperature range. However this may not be strictly true as the optimization is based on approximations obtained from the structural analysis for only one of the reference temperatures (base temperature). However, in all studied cases (Andrade, 2000), the strategy led the optimization process to good results.

Therefore, the great advantage of the optimization strategy presented here resides in the reduced number of solutions of the eigenvalue problem by the subspace iteration technique (Bathe and Wilson, 1976) - one per optimization cycle - in contrast with the technique presented in the previous section, that needs a solution of the

eigenvalue problem for each reference temperature. It is important to point out that all the matrices related to the eigenvalue problem are only calculated once in each structural cycle for both techniques.

Figure (6) also includes the optimization results for approach #3 along with those obtained with the previous techniques. In the curve corresponding to approach #3, the fundamental eigenvalues of the optimal design for the reference temperatures, DT_r, different from the base temperature are computed after the optimization problem is completed. In approach #2 the exact eigenvalues are all available because they were calculated during the structural cycle for all DT_r.

It can be verified in Fig.(6) that the optimal solutions obtained by the two last approaches tend make the plate performance insensitive to the temperature variation. The curve for the optimal design for DT = 0ºC is included for comparison purposes with the other two designs. This curve was chosen because the optimal design for DT = 0ºC incidentally presents low sensitivity to temperature. Also it presents the best performance among all curves presented in Fig.(5).

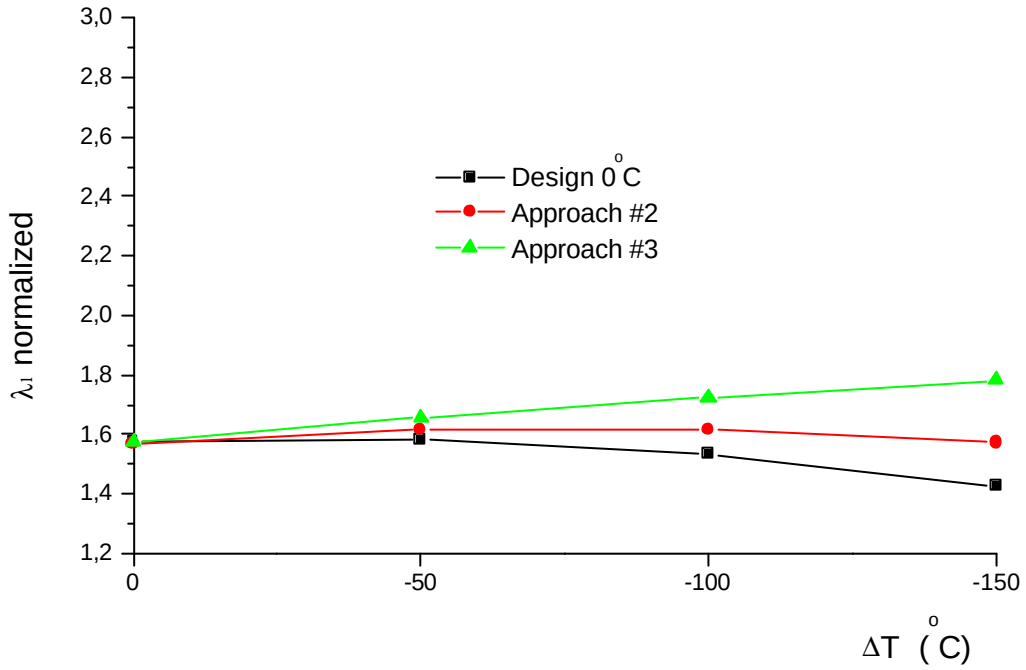

Figure 6 – Optimized plates with the aid of *CMIS*: Approach #2 uses the eigenpairs of the four *DT's*; Approach #3 uses the eigenpairs of DT = -150°C only.

Approach #2 has as optimal design the one computed for the DT at the final cycle. The DT of the objective function in the last cycle is -150ºC. The $l_1^{[ot]}$ of that DT is just an order of 10^{-3} higher than the DT = 0ºC, certifying that the constraints are accurately observed. With this methodology, the problem converged after eleven structural cycles.

In approach #3, the DT_r of the objective function in the last cycle (chosen in the approximate subproblem optimizations) is also -150ºC. But the objective function is about 12% higher than the fundamental eigenvalue for DT = 0ºC (it is one of the approximate constraints in the last cycle), computed by the structural analysis program after the optimization. On the other hand, the convergence occurred after only nine structural cycles.

The following figure illustrates the optimal thickness distribution obtained by approaches #2 and #3. Again, the scale along the *z* axis is 20 time that of the *x* axis. By comparing the thicknesses, it is verified that the designs are quite similar. The stiffeners reduce its thickness the farther they are from the center of the plate. In both cases, reinforcements at 90º exist only at the central strips just as the optimal design obtained for DT = 0ºC, Fig.(4a). The application of the exact constraints, the consideration of all intervals of operation temperature and the *CMIS*, in the Approach #2, provided a finer adjustment of the thickness layers of the stiffeners.

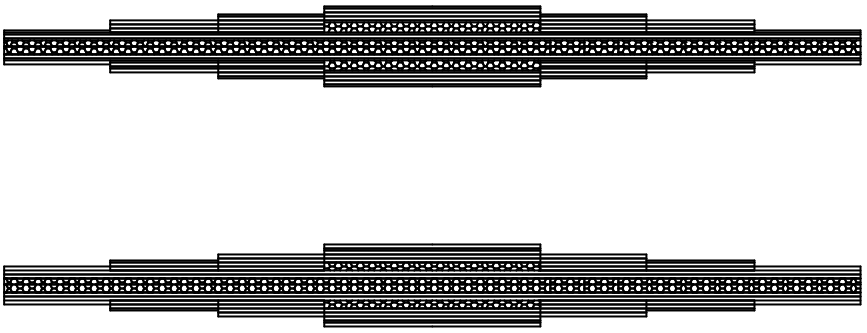

Figure 7 – Thickness distributions for the projects optimized through approach #2 (top) and approach #3 (bottom).

The insensitivity of the design to the temperature does not mean that the optimal design of $DT = 0$ºC (approach #1) is the best design. The result indicates that the optimal design for $DT = 0$ºC provides na upper limit for that temperature and as a lower limit for the other temperatures in the design obtained from approach #2. Also, the insensitivity does not mean that thermal residual stresses does not exist in the optimal plates when $DT_r \neq 0$. Actually, there are alternate areas of tensile and compressive thermal stresses in the plate domain. Figure (8) depicts the thermal stresses in the principal directions at the central integration points of optimal plates obtained from approaches #2 and #3, applied at $DT = -150$ºC. The relative length of the arrows in the two plots is about the same.

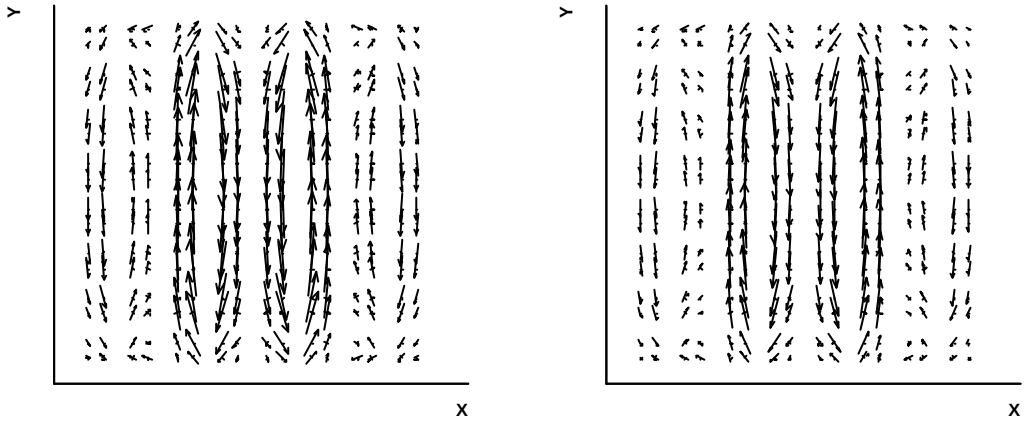

Figure 8 – Distribution of thermal residual stresses in principal directions for $DT = -150^{\circ}$C at Gauss points of each element: left, approach #2; right, approach #3.

It can be observed the almost inexistence of stress resultants along the *x* direction while the stress resultants of neighboring stiffeners have opposite directions. In other words, the central plate stiffeners and the one of the edges are in compression, while the two neighboring stiffeners, inside the plate area, are under tension. It can also be verified that the tensile thermal stress resultants in the plate obtained by approach #2 (exact eigenvectors of all the *DT*'s) are slightly greater than the ones existing in the optimal plate computed from approach #3; also, the magnitude of the stress resultants at the edges of both plates are smaller than at their central areas.

An important advantage of the last two approaches to find the optimum design to operate in a range of temperatures is the reduced number of necessary cycles compared to those needed for optimizations for individual *DT*'s. Eleven and nine structural cycles were necessary for the convergence to the optimal design with approaches #2 and #3, respectively.

It is should be remarked that, within a structural cycle in both approaches, the stiffness and the pre-load geometric matrices are exactly the same for all *DT*'s. The thermal geometric stiffness depend linearly on *DT*. Therefore, it may be computed once and stored for a unit *DT* and multiplied by a constant to obtain their values for different *DT*'s. The proposed approaches are highly efficient.

5. Conclusions

The described strategies were applied with success to optimize a plate with eight variables that are designed to operate within a temperature range. Both approaches were demonstrated to be robust and numerically efficient. The most accurate and safe approach for such purpose is #2: initially, an objective function is chosen at some *DT* to begin the optimization process; approximate eigenvalues constraints are imposed for all *DT´s* with the eigenvectors being accurately computed for all *DT's*. Approach #3 has smaller computacional cost because, in each cycle, it only requires the solution of the eigenvalue problem in a single operation temperature, namely, the base temperature.

It is essential that *CMIS* be used in these approaches. Without this strategy poorer optimal values are obtained as the imposition of eigenvalue constraints (used in the strategy with modal restrictions) does not allow changes neither of the mode nor of *DT* in the objective function. It should be pointed out that the proposed approaches yield safe designs in the whole temperature operation range.

6. References

Almeida, S F. M. and Hansen, J. S., "Enhanced elastic buckling loads of composite plates with tailored thermal residual stresses", *Journal of Applied Mechanics*, Vol. 64, December 1997, pp. 772-780.

Almeira, S. F. M.; Santacreu, A. C. M., "Environmental effects in composite laminates with voids". *Polymers and Polymer Composites*, Vol. 3, Nr. 3, p. 193-204, 1995.

Andrade, L. H., "Otimização de placas laminadas com tensões residuais térmicas em problemas de estabilidade elástica e de freqüências naturais", Doctoral Thesis, Instituto Tecnológico de Aeronáutica, 2002 (in portuguese).

Bathe, K.-J. and Wilson, E. L., "Numerical methods in finite element analysis", Prentice-Hall, Inc., New Jersey, 1976.

Canfield, R. A., "High-quality approximation of eigenvalues in structural optimization", *AIAA Journal*, Vol. 28, Nr. 6, June 1990, pp. 1116-1122.

Hepler, G. R. and Hansen, J. S., "A Mindlin element for thick and deep shells", *Computer Methods in Applied Mechanics and Engineering*, Vol. 54, Nr. 1, Jan 1986, pp. 21-47.

Schmit, L.A. and Miura, H., "Approximation concepts for efficient structural synthesis", NASA CR-2552, 1976.

Thomas, H. L., Vanderplaats, G. N. and Shyy, Y.-K., "A study of move limits adjustments strategies in the approximations concepts approach to structural synthesis", copyright 1992 by VMA Engineering. Published by AIAA, Inc. with permission.

7. Copyright